FABRICATION OF GRADED $Cu(InGa)Se_2$ FILMS BY INLINE EVAPORATION

G.M. Hanket, P.D. Paulson, U. Singh, S.T. Junker†, R.W. Birkmire, F.J. Doyle III†, E. Eser, and W.N. Shafarman
Institute of Energy Conversion, University of Delaware, Newark, DE 19716
†Department of Chemical Engineering, University of Delaware

ABSTRACT

An inline evaporation system for depositing $Cu(InGa)Se_2$ films from elemental sources was characterized. The system demonstrated reproducibly good deposition uniformity and device performance for translation speeds ranging from 1 to 2.5 inches/min. A source effusion model predicting film thickness, composition, and compositional gradients was developed and tested. The effusion model was reasonably successful in predicting measured film characteristics. The model can be further improved by a more accurate description of the flux profiles. In addition, effusion in the transitional flow regime and the possibility of Ga-In interdiffusion need to be explored. Such an improved model would be a valuable tool for the design and development of commercial scale systems, as well as for improved efficiency and flexibility in manufacturing.

INTRODUCTION

Commercial manufacture of $Cu(InGa)Se_2$-based solar modules requires uniform deposition, control of composition, and high throughputs. These requirements can be met by continuous inline evaporation, schematically shown in Fig. 1, in which a heated substrate is linearly translated over sequential Cu, In, and Ga evaporation sources in an Se environment. The potential of inline evaporation has already been demonstrated [1,2].

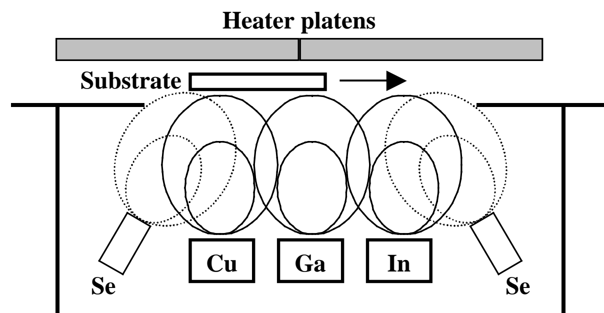

Fig. 1. Schematic of elemental inline evaporation.

The process enables control of the composition and compositional gradients in the film due to the sequential nature of the incident elemental fluxes. This allows the incorporation of Cu-rich transients, which have been shown to improve film properties [3], as well as the grading of the Ga/(Ga+In) ratio in the film, allowing the fabrication of graded-bandgap absorber layers.

A $Cu(InGa)Se_2$ inline evaporation system is being used at the Institute of Energy Conversion (IEC) to develop and verify film deposition models and model-based control strategies that can be used to design and operate commercial-scale systems. The critical modeling issue in an inline evaporation process is the description of the incident fluxes along the direction of substrate translation. The elemental incident fluxes depend on source geometry and temperature and determine the growth rate, overall composition, and instantaneous flux composition at the film surface.

The process control requirements for continuous, extended (> 8 hour) depositions are also being studied. Inline deposition of $Cu(InGa)Se_2$ is inherently problematic to control due to the difficulty in measuring the elemental fluxes at the substrate. Indirect measurements such as source temperature are effective for short-term (1 hour) laboratory depositions, but are unreliable for commercial manufacture. In the IEC system, *in-situ* atomic absorption spectroscopy (AAS) sensors [4] have been installed and are being used to provide element-specific flux measurements. The AAS and source temperature measurements are being incorporated into a model-based process control strategy to improve the accuracy and reliability of the effusion source control.

This paper describes the operational validation of the inline evaporation system and the efforts to model the incident flux profiles through the deposition zone. The operational validation of the system includes deposition uniformity, and reproducibility of run-to-run composition and device performance. A model of the incident flux profiles has been developed based on laboratory scale sources within bell jar systems and has been used to design and describe the $Cu(InGa)Se_2$ film growth in terms of Cu/(Ga+In) development and Ga/(Ga+In) grading. The model is evaluated by comparison to Auger depth profiles of $Cu(InGa)Se_2$ films grown in the system.

EXPERIMENTAL

System Description

The IEC inline evaporation system, shown in Fig. 2, is designed to deposit over a 12" wide web at translation speeds up to 20"/min, presently configured for 6" wide substrates. Each elemental effusion source has two nozzles spaced 4.6" apart. In the standard configuration, the sources are placed 3.5" apart in the sequence Cu-Ga-In, with the Ga source at the halfway point of the deposition zone and the In source closer to the exit side of the zone. The deposition zone is 15" long and is 9.25" above the sources.

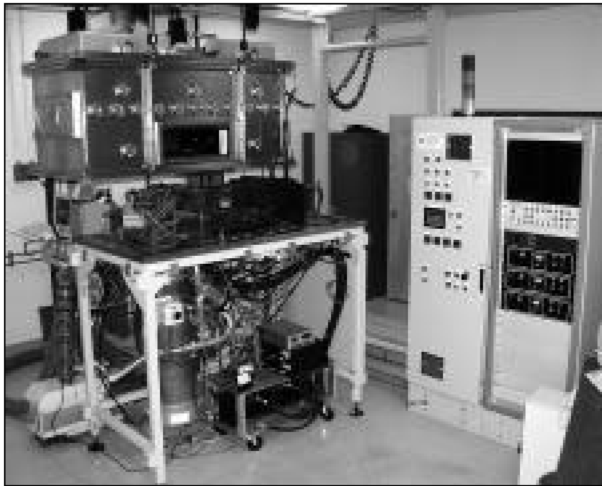

Fig. 2. IEC inline evaporation system.

The substrate is heated by two independently controlled heater platens. The platens are sufficiently longer than the deposition zone so that they heat the substrate before, during, and after deposition. The heater platens are arranged sequentially in order to minimize substrate temperature deviation due to varying thermal radiation from different elemental sources. The substrate temperature is monitored using a bare-junction thermocouple cemented to the substrate surface. The process is housed in a chamber measuring 64"L x 33"W x 27"H. The base pressure is 5×10^{-8} Torr, with a typical operating pressure of 2×10^{-5} Torr.

Temperature control is used for the heater platens and selenium source. Cu, Ga, and In sources are controlled by ATOMICAS™ atomic absorption spectroscopy systems while source temperatures are monitored by thermocouples. Presently, all of the system components are being operated using independent PID control loops.

A model-based control strategy is currently being developed which will integrate multiple sensor measurements and will improve measurement accuracy, reliability, and transient response. Improvement of measurement accuracy and sensor reliability can be achieved through the use of multiple sensors – for example, the use of both AAS and thermocouple measurements for an effusion source. A model-based controller can track both of these measurements, and then estimate the "true" source effusion rate based on the confidence level of each of these measurements. This is especially useful in the case of extended depositions, during which sensor drift may be expected. The use of multiple sensors also allows redundancy in the case of a sensor failure, thereby improving reliability. The transient response of the system can be improved by anticipating the effects of thermal coupling between different system components. An increase in the Cu source power may cause an increase in Ga source temperature or AAS signal. A model-based control system can anticipate the deviation in the Ga source, and appropriately decrease the gallium source power before the deviation occurs.

Approach

Compositional uniformity across the substrate and run-to-run reproducibility of the composition and solar cell results are used to validate the system performance. AES depth profiling data are used to assess the accuracy of the elemental flux modeling.

$Cu(InGa)Se_2$ films were grown on Mo-coated soda lime (SL) glass substrates at substrate temperatures from 425 to 550 ºC and substrate translation speeds from 1 to 2.5 in/min. The films were characterized by thickness, measured by mass gain, and composition, measured by energy dispersive spectroscopy (EDS) and Auger electron spectroscopy (AES). Solar cells were fabricated using a $SL/Mo/Cu(InGa)Se_2/CdS/ZnO/Ni\text{-}Al$ structure with area = 0.5 cm^2 defined by mechanical scribing. The devices were characterized by current-voltage measurements under 100 mW/cm^2 AM1.5 illumination at 25 °C.

RESULTS AND DISCUSSION

System Performance

The compositional uniformity across the 6" wide substrate (in the *cross-direction*) was characterized by EDS measurement. The data, shown in Fig. 3, give uniform Cu/(Ga+In) and Ga/(Ga+In) ratios within the uncertainty of the EDS.

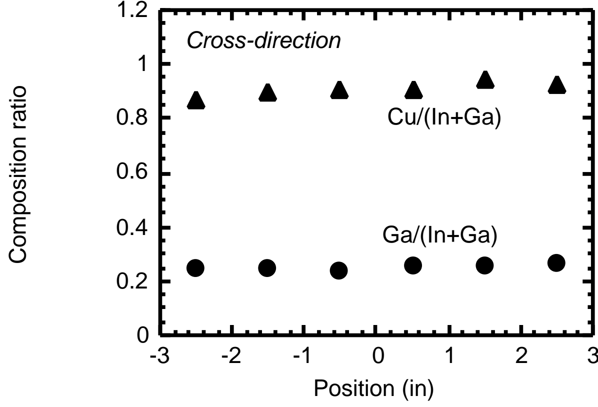

Fig. 3. Compositional uniformity across the deposition zone.

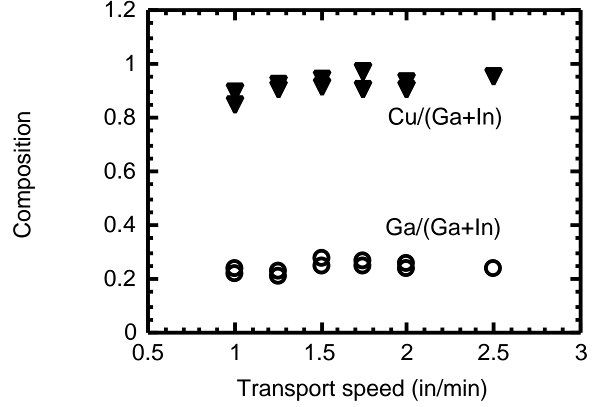

Fig. 4. Composition reproducibility at the center of the substrate over 6 runs with different substrate transport speed.

In order to evaluate the system performance, a number of films were deposited at different substrate translation speeds, from 1"/min to 2.5"/min. The source effusion rates were held constant, so that the films would vary in thickness but retain a fixed composition. Film composition was characterized by EDS and the film quality by the performance of solar cells fabricated from them. Fig. 4 shows the film composition at the center of the substrate, and indicates good run-to-run reproducibility. The best solar cell result from each run is shown in Table 1, again indicating good system reproducibility as well as high film quality in terms of device performance over a 2.5 times range of deposition rates. It should be noted that, with respect to film thickness, the drop in performance for thickness < 1µm is consistent with the work of Negami et al. [5]. The best device produced in the system to date had V_{OC} = 0.606 V, J_{SC} = 33.2 mA, FF = 74.3%, and eff. = 14.9% under 100mW/cm^2 AM1.5 illumination.

In summary, the system is capable of depositing uniform, device quality $Cu(InGa)Se_2$ films at relatively high deposition rates.

Process Modeling

A quantitative description of the incident fluxes at the substrate is necessary to model the inline deposition of $Cu(InGa)Se_2$ films. A model of the deposition onto a moving substrate from a multi-nozzle evaporation source was previously reported for the case of large-area CdS deposition [6]. In that case, the flux composition inherently maintained the correct stoichiometry since CdS evaporates congruently. However, modeling of $Cu(InGa)Se_2$ film growth from elemental sources requires a quantitative description of the spatial distribution of multiple elemental fluxes.

Table 1. Device performance with increasing translation speed.

Speed (in/min)	Thickness (µm)	V_{OC} (V)	J_{SC} (mA/cm^2)	FF (%)	Eff (%)
1	2.1	0.594	32.1	69.4	13.2
1.25	2	0.594	32.5	71.8	13.8
1.5	1.8	0.614	33.2	71.7	14.6
1.75	1.4	0.588	33.7	70.5	14.0
2	1.3	0.590	33.6	67.8	13.5
2.5	0.9	0.570	31.9	66.3	12.2

The source geometry used for the model is shown in Fig. 5 where the vector (,) points from the source to a given point on the substrate. The flux profile the effusion source can be approximated using:

$$f(\, , \,) = \frac{F(n+1)}{2 \quad ^2} \cos^n \qquad \text{(Eq. 1)}$$

where n is an empirical fitting parameter describing the beaming of the molecular beam. In the case of free-molecular flow, the molecular beam profile is solely a function of the nozzle aspect ratio (nozzle length divided by nozzle diameter) [7]. The accumulation rate, f^{dep}, at the substrate is obtained by multiplying Eq. 1 by an additional cos correction to account for the angle of incidence. F is the effusion rate from the source and, again for free-molecular flow, can be approximated by [8]:

$$F = \quad ^2 K(p_1 - p_2)\sqrt{\frac{M}{2 \quad RT}} \qquad \text{(Eq. 2)}$$

where is the nozzle radius, p_1 is the partial pressure inside the source and is approximately the saturation pressure, p_2 is the partial pressure in the chamber and is

negligible compared to p_1, and K is an empirical function of the nozzle aspect ratio which typically varies from 1 to 0.1 [9]. The deposition from multiple sources at a point on the substrate is calculated by simply summing the individual source contributions.

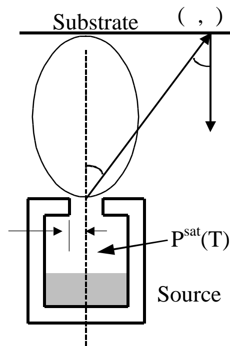

Fig. 5. Variables used in effusion analysis.

The measured film thickness profiles for a Cu film deposited onto a large-area (16" x 14"), stationary substrate are shown in Figs. 6 and 7 for the cross-direction and the *machine-direction* (along the direction of substrate translation), respectively. The flux as represented by the thickness at the substrate edges (+3 and –3 inches) is 10-15% less than the flux at the center, giving a thickness uniformity of ±5-7%. The data were fit by using Eq. 1 for each source nozzle, with n as the fitting parameter. The best fit, shown as the solid lines in Fig. 6 and 7, was obtained for n = 4.9. Fig. 7 also shows the relative error between the fit and the data. The predicted profile is within the bounds of published effusion profiles for nozzles with similar aspect ratios [10]. Since the molecular beam profile only depends on nozzle geometry in the free-molecular flow regime, the flux profile measured for Cu is assumed to apply to the Ga and In sources as well.

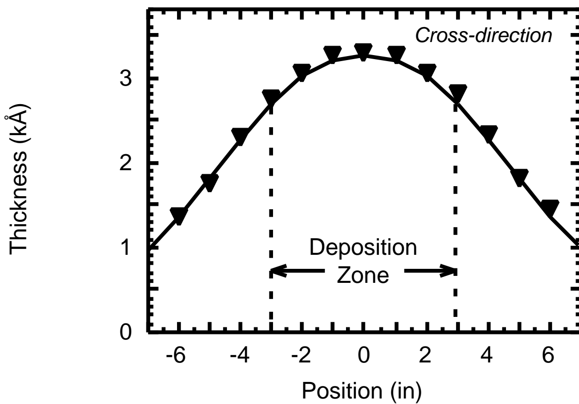

Fig. 6. Cu thickness profile across the deposition zone.

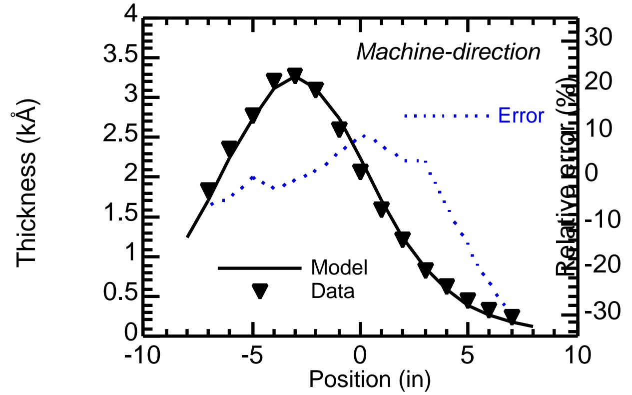

Fig. 7. Cu thickness profile along the deposition zone length.

Elemental incident fluxes calculated from the model are shown in Fig. 8 for a typical film grown at a substrate speed of 1"/min. These profiles are used to predict the film growth rate and composition gradings in the growing film. Fig. 9 shows the modeled profile and demonstrates how the inline system mimics a "two-stage" growth process (Cu-rich to Cu-poor) as the substrate moves through the deposition zone. The film is Cu-rich through nearly the whole of the deposition. The film reaches its target Cu/(Ga+In) ratio of 0.85 within only an inch or so of the deposition zone exit.

The model was used to predict the compositional depth profiles of $Cu(InGa)Se_2$ films. Fig. 10 shows the Auger depth profile of a $Cu(InGa)Se_2$ film grown at 1"/min and substrate temperature of 525 °C. The data show a flat Cu profile, unlike that shown in Fig. 9, indicating Cu homogenization, giving evidence for high Cu mobility. Also, the Cu/(Ga+In) ratio from the Auger data compares quite well to the endpoint value of the model-predicted Cu/(Ga+In) ratio in Fig. 9. The data also show that Ga and In retain a grading consistent with their sequence of deposition – that is, Ga-rich near the Mo interface, In-rich near the surface.

Assuming negligible Ga-In interdiffusion, a Ga/(Ga+In) profile can be predicted by simply plotting the incident Ga/(Ga+In) flux against the film thickness as the substrate is translated through the deposition zone. The Ga/(Ga+In) profile is essentially modeled as a "history" of the incident flux composition.

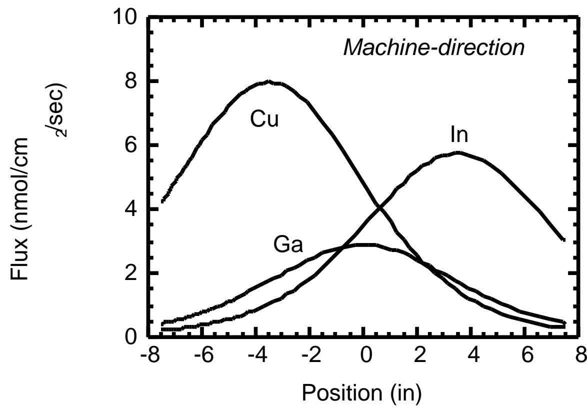

Fig. 8. Predicted elemental flux profiles along deposition zone centerline in machine direction.

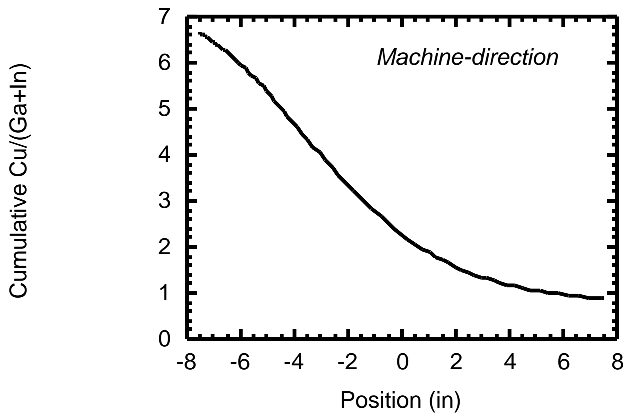

Fig. 9. Predicted Cu/(Ga+In) development as the substrate moves through the deposition zone.

AES profiles for Ga/(Ga+In) in films deposited at 450 and 525 °C, are compared to model predictions in Fig.s 11 and 12, respectively. Error bars of 0.08 on the Ga/(Ga+In) data are estimated, based on a 1 atomic % error in the Ga and In compositions measured by AES.

The model prediction is reasonable for the front of the films (z > 1 μm), but overpredicts the Ga content at the back of the films (Mo interface). This discrepancy between model and experiment was found to increase with increased separation between the Ga and In sources.

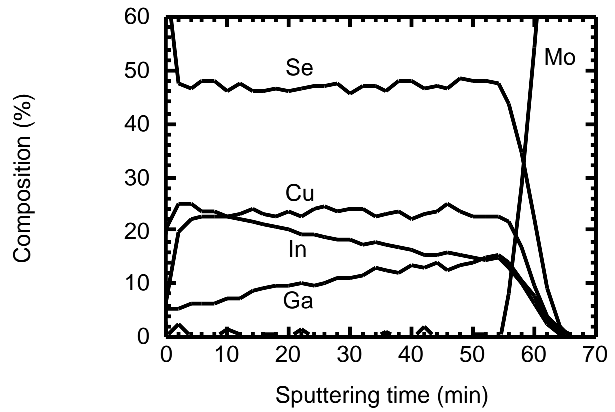

Fig. 10. AES depth profile of $Cu(InGa)Se_2$ film deposited at 525°C and 1"/min.

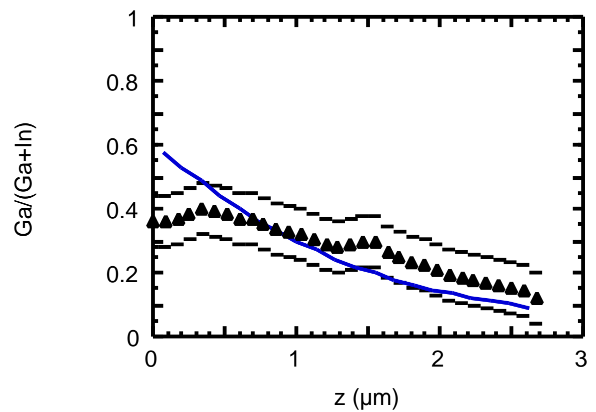

Fig. 11. Modeled (solid line) and measured Ga profile of film grown at T_{SS} = 450 °C.

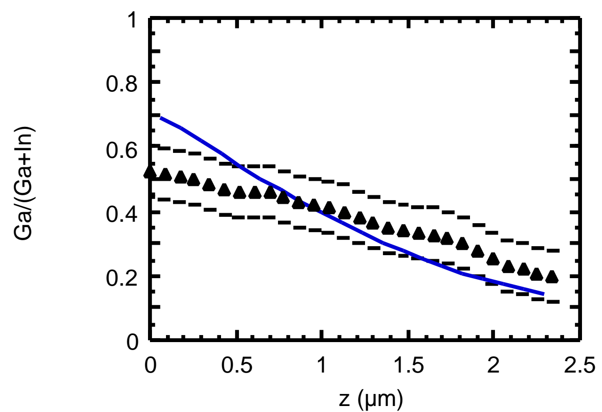

Fig. 12. Modeled (solid line) and measured Ga profile of film grown at T_{SS} = 525 °C.

There are two possible explanations for the model's overestimation of the Ga/(Ga+In) ratio at the back of the film: an inaccuracy in the model itself, or possible Ga-In interdiffusion in the growing film.

There are two possible errors in the flux model. The first is the use of a $\cos^n$ functionality to fit the experimental data. As can be seen from Fig.7, the $\cos^{4.9}$ flux profile underestimates the thickness by 30% at a distance of 10" from the source in the machine direction. In the standard source configuration, the In source is located 10" away from the deposition zone entrance. As a result, the Ga/(Ga+In) ratio is overestimated by the model. Clearly, the discrepancy between the model and experiment would increase as the In source is moved further away from the zone entrance.

The second error in the flux model could be due to the assumption of free-molecular flow, and hence identical flux profiles, for the various elemental sources. For these experiments, all of the sources operated near a Knudsen number of 1, the boundary between free-molecular and transitional flow. As the flow moves into the transitional regime, the flux profile becomes more diffuse [11]. Indium would be the most likely to cross over into the transitional flow regime, as it has the largest atomic diameter and is therefore more likely to experience vapor-phase collisions. If this were to happen, the indium flux would increase at the deposition zone entrance, thereby reducing the Ga/(Ga+In) ratio at the back of the film. The present flux model may need to be refined and verification of the flux model will likely require independent calibrations of the Ga and In sources.

Ga-In interdiffusion may also play a role in controlling the Ga/(Ga+In) grading in the film. Such interdiffusion in $Cu(InGa)Se_2$ films is known to occur and has been characterized [12, 13].P

CONCLUSIONS

An inline evaporation system for the deposition of $Cu(InGa)Se_2$ films has been put into operation at IEC. The system's performance in terms of uniform deposition over large areas at relatively high rates and in terms of film quality as determined by device results has been successfully demonstrated. Also demonstrated was the system's run-to-run reproducibility in terms of the same benchmarks.

A preliminary flux model has been developed which predicts the elemental incident fluxes based on the system geometry and source effusion rates. The model can be used to predict film growth rate, uniformity, composition, and compositional gradients in the film. Efforts to validate the model by comparison to AES measurements of Ga/(Ga+In) profiles were moderately successful and can further be improved by a more accurate description of the molecular beam profiles. In addition, effusion in the transitional flow regime and the possibility of Ga-In interdiffusion need to be explored. Such an improved model is a valuable tool for commercial scale-up, as well as for improved efficiency and flexibility in manufacturing. An accurate and reliable flux model is also necessary for the study and development of bandgap-engineered absorber materials, adhesion-promoting interlayers, and the development of new and chemically more complex absorber systems.

ACKNOWLEDGMENTS

This work was supported by National Renewable Energy Laboratory under subcontract no. ZAK-8-17619-33, Global Solar Energy, LLC, ITN Energy Systems and the State of Delaware Research Partnership Program. Special thanks to Amy Swartzlander, NREL, for Auger analysis.

REFERENCES

1. E. Niemi, J. Hedström, T. Martinsson, K. Granath, L. Stolt, J. Skarp, D. Hariskos, M. Ruckh, and H. W. Schock, *25th IEEE Photovoltaic Specialists Conference*, 801 (1996).
2. M. Powalla, G. Voorwinden, and B. Dimmler, *14th European Photovoltaic Solar Energy Conference*, 1270 (1997).
3. W. E. Devaney, W. S. Chen, J. M. Stewart, and R. A. Mickelsen, *IEEE Trans. Elec. Devices* **37**, 428 (1990).
4. C. Lu and Y. Guan, *J. Vac. Sci. Tech. A* **13(3)**, 1797 (1995).
5. T. Negami, S. Nishiwaki, Y. Hashimoto, N. Kohara, and T. Wada, *2nd World Conference and Exhibition on Photovoltaic Solar Energy Conversion*, 1181 (1998).
6. R. E. Rocheleau, Ph. D. Dissertation, University of Delaware (1981).
7. P. Clausing, *Z. Phys.* **66**, 471 (1930).
8. R.E Rocheleau, B.N. Baron, and T.W.F. Russell, *AIChE Journal* **28(4)**, 656 (1982).
9. E.H. Kennard, *Kinetic Theory of Gases*, McGraw-Hill Book Co., New York, 306 (1938).
10. L. Valyi, *Atom and Ion Sources*, John Wiley & Sons, London, 86 (1977).
11. S.C. Jackson, B.N. Baron, R.E. Rocheleau, and T.W.F. Russell, *J. Vac. Sci. Tech. A* **3(5)**, 1916 (1985).
12. D.J. Schroeder, G.D. Berry, and A.A. Rockett, *Appl. Phys. Lett.* **69(26)**, 4068 (1996).
13. M. Marudachalam, R.W. Birkmire, H. Hichri, J.M. Schultz, A. Swartzlander, and M.M. Al-Jassim, *J. Appl. Phys.* **82(6)**, 2896 (1997).